ELSEVIER

Applied Surface Science 112 (1997) 38–47

applied surface science

Molecular layer epitaxy by real-time optical process monitoring

K.J. Bachmann [a,*], C. Höpfner [a], N. Sukidi [a], A.E. Miller [a], C. Harris [a], D.E. Aspnes [b], N.A. Dietz [b], H.T. Tran [c], S. Beeler [c], K. Ito [c], H.T. Banks [c], U. Rossow [d]

[a] *Department of Materials Science and Engineering, North Carolina State University, Raleigh, NC 27695-7919, USA*
[b] *Department of Physics, North Carolina State University, Raleigh, NC 27695-7919, USA*
[c] *Department of Mathematics, North Carolina State University, Raleigh, NC 27695-7919, USA*
[d] *Fachbereich Physik, Technische Universität Berlin, Berlin, Germany*

Abstract

In this paper we consider modern methods of optical process monitoring and control in the context of atomic layer epitaxy. One specific method, p-polarized reflectance spectroscopy (PRS), is chosen to assess details of layer-by-layer growth. We show that PRS monitoring under conditions of steady-state growth by pulsed chemical beam epitaxy (PCBE) can achieve the deposition of molecular layers of GaP on silicon (100) deposited with a precision of 5%, which can be improved by reducing the growth rate and increasing the period of time averaging of the reflectance data. Since in the nucleation period prior to formation of a contiguous heteroepitaxial film inhomogeneous surface chemistry and roughening complicates the modeling of the overgrowth process, advances in both experimental methods and theory are required for extending the control to non-steady-state growth conditions. Results of simultaneous single-wavelength PR monitoring and laser light scattering measurements in conjunction with atomic force microscopy studies of short period heteroepitaxial overgrowth processes are presented. The extension of PRS to the monitoring of organometallic chemical vapor deposition at higher pressures is also discussed.

1. Introduction

So far atomic layer epitaxy (ALE) has relied on self-limiting mechanisms, which may generate either growth of one atomic layer at a time [1–3] or more complex mechanisms of layer-by-layer deposition [4]. The engineering of layer-by-layer epitaxy through closed-loop feedback control using real-time optical process monitoring represents a possible avenue for the realization of layer-by-layer growth without reliance on a chemical self-limiting mechanism. A variety of methods for real-time optical monitoring of the rate of epitaxial processes have been developed, such as, near normal incidence reflectance [5,6], p-polarized reflectance (PR) [7,8] and spectroscopic ellipsometry (SE) [9–11]. Both PR and SE have demonstrated the ability to resolve submonolayer deposition features. Thus far, SE is the only method for which sample-driven control of

* Corresponding author. Materials Research Center, Research Bldg. 1, Room 219, Centennial Campus, North Carolina State University, Raleigh, NC 27695-7919, USA. Tel.: +1-919-5152538; fax: +1-919-5153419; e-mail: bachmann@mte.ncsu.edu.

PII S0169-4332(96)00975-0

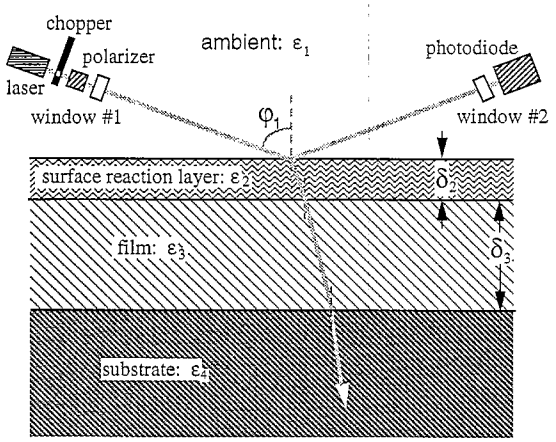

Fig. 1. Schematic representation of the reflection of a p-polarized laser beam by a four layer stack: (1) ambient, (2) surface reaction layer, (3) epilayer and (4) substrate.

composition has been demonstrated [12], to a precision of 3% for a layer thickness of 3 Å [12]. The objective of this paper is to assess the utility of real-time monitoring by PR measurements for the control of layer-by-layer growth, using the heteroepitaxial growth of GaP on Si(100) by pulsed chemical beam epitaxy (PCBE) as an illustrative example.

2. Real-time monitoring of GaP CBE on Si(100) by p-polarized reflectance

In PCBE of GaP on Si(100), the substrate wafer, held at a temperature of typically 623 K, is exposed to a train of sequential pulses of source vapor molecules e.g. triethylgallium (TEG) and tertiary-butylphosphine (TBP) [13]. The experimental arrangement is described in detail elsewhere [14,16–18]. For single-wavelength PR monitoring, a chopped laser beam e.g. a HeNe laser beam at 632.8 nm wavelength, is polarized by a Glan–Thompson prism to an s- and p-polarized intensity ratio $I_s/I_p = 10^{-6}$, and is reflected on the surface of the wafer and phase sensitively detected. When a highly p-polarized laser beam of wavelength λ impinges at angle of incidence ϕ_1 onto the interface between two media of dielectric functions $\varepsilon_1(\lambda) = \varepsilon_{1r}(\lambda) + i\varepsilon_{1i}(\lambda)$ and $\varepsilon_2(\lambda) = \varepsilon_{2r}(\lambda) + i\varepsilon_{2i}(\lambda)$, a minimum value of the reflectance $R_p(\phi_1)$ is observed for $\phi_1 = \phi_{pB}$, the pseudo-Brewster angle of the interface. The pseudo-Brewster angle satisfies the following cubic polynomial:

$$2(p^2+q)v^3 + p^2(p^2-3)v^2 - 2p^4v + p^4 = 0, \tag{1}$$

where $v = \sin^2\phi_{pB}$, $p = |\varepsilon_2|$ and $q = \varepsilon_{2r}$ [19]. For a silicon/vacuum interface, at room temperature and $\lambda = 632.8$ nm, $\phi_{pB} = 75.637°$ and $R_p(\phi_{pB}) \approx 10^{-5}$, depending on conditions discussed in more detail below.

Recently, we have shown [17,18] that a four-layer stack consisting of: (1) ambient, (2) surface reaction layer (SRL), (3) epitaxial film and (4) substrate, is the simplest possible representation of chemical vapor deposition of a heteroepitaxial film. Fig. 1 shows schematically the reflection of a p-polarized laser beam on a four-layer stack, which for chemical beam epitaxy of GaP/Si heterostructures consists of: vacuum, SRL, GaP and Si. The SRL is composed of molecules, molecular fragments and atoms that are generated on the surface of the solid by pyrolysis of the source vapor molecules and subsequent chemical reactions among the products. The complex reflectivity coefficient r_p for a four-layer stack is given by

$$r_p = \{r_{12} + r_{23}\exp(-2i\beta_2) + [r_{12}r_{23} + \exp(-2i\beta_2)]r_{34}\exp(-2i\beta_3)\}$$
$$/\{1 + r_{12}r_{23}\exp(-2i\beta_2) + [r_{23} + r_{12}\exp(-2i\beta_2)]r_{34}\exp(-2i\beta_3)\}, \tag{2}$$

where the Fresnel coefficients $r_{k(k+1)}$ $(k = 1, 2, 3)$ for the interfaces 12, 23 and 34 are given by

$$r_{k(k+1)} = \left(\varepsilon_{k+1}\sqrt{\varepsilon_k - \varepsilon_1 \sin^2 \phi_1} - \varepsilon_k\sqrt{\varepsilon_{k+1} - \varepsilon_1 \sin^2 \phi_1} \right) \Big/ \left(\varepsilon_{k+1}\sqrt{\varepsilon_k - \varepsilon_1 \sin^2 \phi_1} + \varepsilon_k\sqrt{\varepsilon_{k+1} - \varepsilon_1 \sin^2 \phi_1} \right) \quad (3)$$

and the phase angles β_k for the SRL $(k = 2)$ and the growing epilayer $(k = 3)$ are given by

$$\beta_k = \frac{2\pi\delta_k}{\lambda}\sqrt{\varepsilon_k - \varepsilon_1 \sin^2 \phi_1}\,. \quad (4)$$

δ_k $(k = 2, 3)$ refers to the thicknesses of the surface reaction layer and epilayer, respectively, and ε_1, ε_2, ε_3 and ε_4 refer to the dielectric functions of the ambient, surface reaction layer, heteroepitaxial film and substrate, respectively, at wavelength λ of the incident laser beam.

Due to interference of the partial waves reflected at the ambient/SRL, SRL/epilayer and epilayer/substrate interfaces, the reflectivity $R_p = r_p r_p^*$ oscillates, as illustrated for the case of pulsed CBE of GaP on Si(100) substrate wafer in Fig. 2(a). Two distinct superimposed oscillations are observed: a slowly varying oscillation of large amplitude with a period of $\Delta t_m = 650$ s and a fine structure with a period of 3 s that is magnified and shown as an inset in Fig. 2(a). The fine structure has same periodicity t_{svc} as the source vapor pulse cycles employed in the pulsed CBE process as illustrated in Fig. 2(b).

Since the amplitude of the fine structure associated with the periodic changes in composition and thickness of

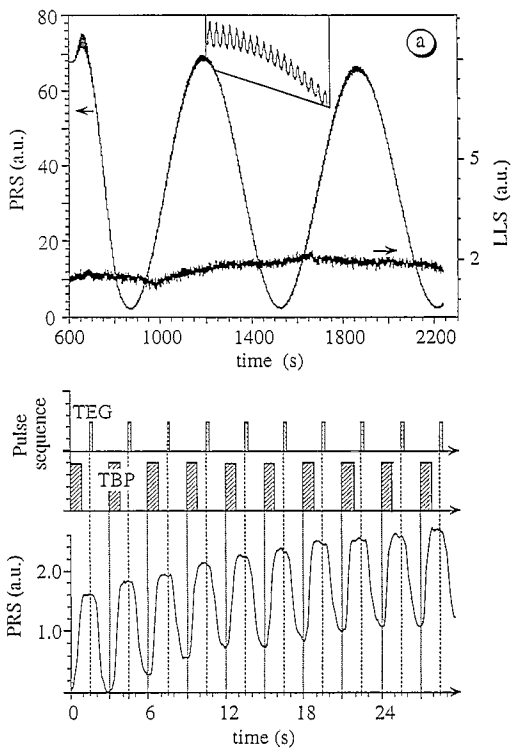

Fig. 2. (a) Plot of the PR intensity (left ordinate) and scattered light intensity (right ordinate) versus time for GaP heteroepitaxy on Si(100). (b) Correlation of pulse sequence and fine structure in the PR intensity.

the SRL is small compared to the amplitude of the interference oscillations, Eq. (2) can be simplified by linearization with respect to phase angle β_2 [20], that is

$$r_p \approx r_{po} + \beta_2 \left.\frac{\partial r_p}{\partial \beta_2}\right|_{\beta_2=0}, \tag{5}$$

where $r_{po} = r_p(\beta_2 = 0)$. For $\beta_2 = 0$, $r_{12} = 0$, $\delta_2 = 0$ and $\lim_{\delta_2 \to 0} r_{23} = r_{13}$, so that

$$r_{po} = \frac{r_{13} + r_{34}e^{-i2\beta_3}}{1 + r_{13}r_{34}e^{-i2\beta_3}} \tag{6}$$

For the general case of $r_{13} = r_{13r} + ir_{13i}$, $r_{34} = r_{34r} + ir_{34i}$ and $\beta_3 = \beta_{3r} + i\beta_{3i}$,

$$\begin{aligned} R_{po} = {} & \{|r_{13}|^2 + |r_{34}|^2 \exp(4\beta_{3i}) \\ & + [2(r_{13r}r_{34r} + r_{13i}r_{34i})\cos(2\beta_{3r}) + 2(r_{13r}r_{34i} - r_{13i}r_{34r})\sin(2\beta_{3r})]\exp(2\beta_{3i})\} \\ & / \{1 + |r_{13}|^2|r_{34}|^2 \exp(4\beta_{3i}) + [2(r_{13r}r_{34r} - r_{13i}r_{34i})\cos(2\beta_{3r}) \\ & + 2(r_{13r}r_{34i} + r_{13i}r_{34r})\sin(2\beta_{3r})]\exp(2\beta_{3i})\} \end{aligned} \tag{7}$$

For a stack: (1) ambient, (3) transparent film and (4) absorbing substrate, Eq. (7) simplifies to:

$$\begin{aligned} R_{po} = {} & \{r_{13r}^2 + |r_{34}|^2 + 2r_{13r}[r_{34r}\cos 2\beta_{3r} + r_{34i}\sin 2\beta_{3r}]\} \\ & / \{1 + r_{13r}^2|r_{34}|^2 + 2r_{13r}[r_{34r}\cos 2\beta_{3r} + r_{34i}\sin 2\beta_{3r}]\}, \end{aligned} \tag{8}$$

which for $\phi_1 = \phi_{pB}$ has minimum at

$$\delta_3(n) = \frac{[n + 2\gamma]\lambda}{2\sqrt{\varepsilon_3 - \varepsilon_1 \sin^2 \phi_B}} \tag{9}$$

where $n = 0, 1, 2, \ldots$ and γ refers to a shift in the position of the minima due to $\varepsilon_{4i} \neq 0$. The spacings in film thickness between successive minima in the interference oscillations

$$\Delta\delta_{3m} = \delta_{3m}(n) - \delta_{3m}(n-1) = \frac{\lambda}{2\sqrt{\varepsilon_3 - \varepsilon_1 \sin^2 \phi_{B4}}} \tag{10}$$

correspond to period Δt_m in time. Thus for the specific example of GaP growth on Si(100) given in Fig. 2, where $\lambda = 632.8$ nm, $\Delta t_m = 650$ s and $\Delta\delta_{3m} \approx 101$ nm, the average growth rate $\bar{v}_{g3} = \Delta\delta_3/\Delta t_m \approx 1.6$ Å/s. With source vapor cycle time $t_{svc} = 3$ s the average change in thickness per source vapor cycle is $\Delta\bar{\delta}_3 = 4.8$ Å, that is, corresponds to more than one molecular layer of GaP in this particular experiment.

3. Formulation of control problem and error analysis for steady-state growth

In general the experimentally established instantaneous growth rate $v_{ge}(t)$ and increments in the epilayer thickness per source vapor cycle $\Delta\delta_{3e}(t) = v_{ge}(t) \cdot t_{svc}$ are expected to deviate from the desired values. For molecular layer epitaxy of GaP on Si(100) the desired thickness is precisely one molecular layer per cycle, corresponding to $\Delta\delta_3 = 2.726$ Å at room temperature, that is, for $t_{svc} = 3$ s, $v_g(t) = 0.91$ Å/s. The control of molecular layer deposition is implemented by evaluating the deviation between the theoretically predicted slope

$$S_p = \frac{\partial R_{po}}{\partial t} = \frac{-4r_{13}(r_{34r}\sin 2\beta_3 - r_{34i}\cos 2\beta_3)(r_{13}^2 - 1)(|r_{34}|^2 - 1)}{(1 + r_{13}^2|r_{34r}|^2 + 2r_{13}(r_{34r}\cos 2\beta_3 + r_{34i}\sin 2\beta_3))^2}\left(\frac{\partial\beta_3}{\partial t}\right), \tag{11}$$

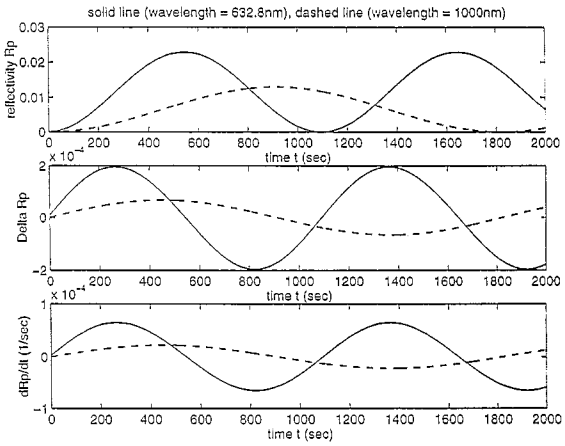

Fig. 3. Plot of the reflectivity, step height in the reflectivity and slope of the interference oscillations for pulsed GaP growth on Si(100) versus time, incrementing the epilayer by exactly one molecular layer per source vapor cycle.

and the experimentally determined slope $S_e = \Delta R_{poe}(t)/t_{svc}$. Utilizing this deviation to generate a control signal the source vapor flux and/or substrate temperature are adjusted to minimize $|\Delta S|^2 = |S_p - S_e|^2$. Fig. 3 shows a plots of $R_{po}(t)$, $\Delta R_{po}(t) = t_{svc} \cdot [\partial R_{po}(t)/\partial t]$ and $\partial R_{po}(t)/\partial t$ versus time for molecular layer growth of GaP on Si(100) using the following input parameters: $\Delta\delta_3 = 2.726$ Å, $\varepsilon_1 = 1$, $\varepsilon_3 = 10.96$, $\varepsilon_4 = 15.25 + 0.17\mathrm{i}$ and $\phi_{pB} = 75.64°$ at $\lambda_1 = 632.8$ nm and $\varepsilon_1 = 1$, $\varepsilon_3 = 10.05$, $\varepsilon_4 = 12.92$ and $\phi_{pB} = 74.45°$ at $\lambda_2 = 1000$ nm [21,22].

The precision with which ΔS can be determined depends on the precision of the measurements of $\Delta R_{poe}(t)$ and t_{svc}. The former depends on the noise $\Delta\bar{R}_{po}$ due to intensity variations in the laser beam and noise generated in signal processing as well as random errors in $\varepsilon(T)$ due to fluctuations of the substrate temperature, which is $\leq \pm 1°$. Note that a random error in ε_3 results in a random error in ϕ_{pB}, so that at constant ϕ_1,

$$\frac{\delta R_{poe}(\varepsilon, \phi_1, \Delta\bar{R}_{po})}{R_{po}} = \sqrt{\left(\frac{1}{R_{po}}\frac{\partial R_{po}}{\partial\varepsilon}\Delta\varepsilon\right)^2 + \left(\frac{1}{R_{po}}\frac{\partial R_{po}}{\partial\phi_1}(\phi_1 - \phi_{pB})\right)^2 + \left(\frac{\Delta\bar{R}_{po}}{R_{po}}\right)^2}. \tag{12}$$

To calculate the error in measuring S_e we observe that

$$R_{poe}(t_i) = R_{po}(t_i \pm \delta t_i) \pm \delta R_{poe}(t_i) \tag{13}$$

where $R_{poe}(t_i)$ is the measured value of R_{poe} at time t_i at the start of the ith source vapor cycle and $R_{po}(t_i \pm \delta t_i)$ is the exact value of the reflectivity at time $t_i \pm \delta t_i$ with δt_i being the timing error. Since δt_i is small, Taylor series expansion of the term $R_{po}(t_i \pm \delta t_i)$ yields

$$R_{poe}(t_i) \approx R_{po}(t_i) \pm \frac{\partial R_{po}(t_i)}{\partial t}\delta(t_i) \pm \delta R_{poe}(t_i). \tag{14}$$

Similarly at time t_{i+1} at the end of the ith source vapor cycle we have

$$R_{poe}(t_{i+1}) \approx R_{po}(t_{i+1}) \pm \frac{\partial R_{po}(t_{i+1})}{\partial t}\delta(t_{i+1}) \pm \delta R_{poe}(t_{i+1}) \tag{15}$$

Upon subtracting Eq. (14) from Eq. (15) and dividing by t_{svc} we get

$$\frac{R_{poe}(t_{i+1}) - R_{poe}(t_i)}{t_{svc}} \approx \frac{R_{po}(t_{i+1}) - R_{po}(t_i)}{t_{svc}} \pm \delta S_e. \tag{16}$$

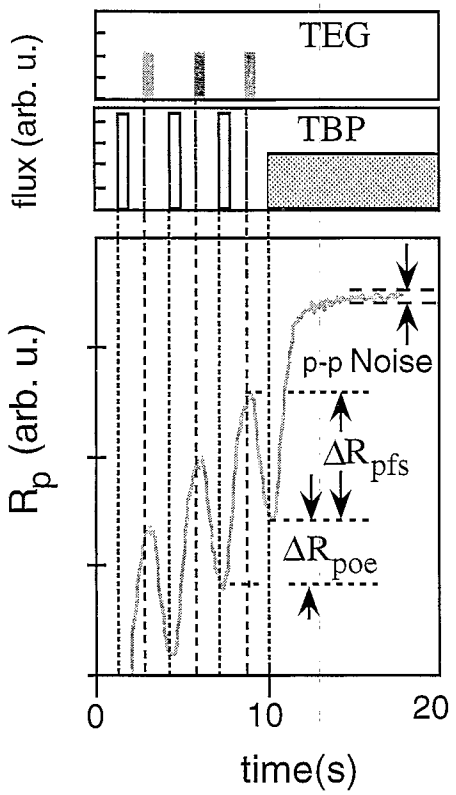

Fig. 4. Experimentally determined step height ΔR_{poe} due to growth, fine structure amplitude ΔR_{pfs} and peak-to-peak noise amplitude under the conditions of interrupted steady-state growth under conditions of constant TBP flux.

δS_e is the error in the measured slope S_e and is given by

$$\delta S_e = \frac{1}{t_{svc}}\left(\delta R_{poe}(t_{i+1}) - \delta R_{poe}(t_i) + \frac{\partial R_{po}(t_{i+1})}{\partial t}\delta t_{i+1} - \frac{\partial R_{po}(t_i)}{\partial t}\delta t_i\right) \tag{17}$$

If the errors $\delta R_{poe}(t_i)$ and δt_i are independent, the variance of S_e is given by

$$\mathrm{var}(S_e) = \frac{1}{t_{svc}^2}\left\{\mathrm{var}\left[R_{poe}(t_{i+1})\right] + \mathrm{var}\left[R_{poe}(t_i)\right] + \left(\frac{\partial R_{po}(t_{i+1})}{\partial t}\right)^2 \mathrm{var}[t_{i+1}] + \left(\frac{\partial R_{po}(t_i)}{\partial t}\right)^2 \mathrm{var}[t_i]\right\} \tag{18}$$

Using the random error in switching time specified by the supplier of the valves used in our CBE system, we calculate the variance of t_i to be 2.5×10^{-3} s^2. The variance in R_{poe} can be determined from the noise measured under conditions of interrupted steady state growth in the presence of a stabilizing TBP beam, as illustrated in Fig. 4 and is 4.9×10^{-11}. The largest value of $\Delta R_{poe} = 2 \times 10^{-4}$ so that at $t_{svc} = 3$ s the maximum slope is $S_{emax} = 6.7 \times 10^{-5}$ s^{-1}. Therefore, the variance of S_e is 1.416×10^{-11}, which results in a precision of 5.9% for the specific example considered here. By Eq. (18), the precision can be improved by simultaneously increasing t_{svc} and decreasing v_g so that $\Delta\delta_3$ remains unchanged. At the low processing temperature of PCBE, the rate of decomposition of TEG is slow, so that, at the short source vapor cycles times employed thus far, a carry-over of TEG fragments ensues from one cycle into the next. This complicates the

response to adjustments in the source vapor flux imposed by the control signal and reinforces the need for longer source vapor cycles. For example, choosing $t_{svc} = 10$ s and extending the period of time averaging of the measured reflectivity data from 300 ms to 1.5 s reduces δR_{pe} by a factor of 1.8 and results in a variance of S_e of 5.64×10^{-13}. For a maximum slope of 2×10^{-5} s^{-1}, this results in a precision of 3.8%, for the set of valves used in our work. Reductions of the error in the switching time by a factor of 5 are possible with existing technology. Thus similar precision should be possible for the use of PR in controlling layer thickness as achieved by SE. Also, for materials combinations exhibiting larger differences between ε_3 and ε_4 (e.g. CaF_2/Si or CeO_2/Si heterostructures) significantly larger values of R_{po} and larger slopes are observed, which should facilitate the engineering of molecular layer epitaxy for selected materials systems.

Systematic errors in the experimentally observed steps $\Delta R_{poe}(t)$ are introduced by depolarization, divergence of the incident laser beam and limited accuracy in setting the growth temperature. In a small angular range $\phi_{pB} \pm \Theta$ about the pseudo-Brewster angle the reflectance is a parabolic function of angular deviation, that is

$$R_{poe}(\phi) = R_{po}(\phi_{pB}) + \frac{\Delta R_{po}}{\Theta^2} \Delta\phi^2, \tag{19}$$

where $\Delta R_p = R_p(\Theta) - R_p(\phi_B)$ and $\Delta\phi_1 = \phi_1 - \phi_{pB}$. By integration over the range of angular divergence of the laser beam $2\alpha \in [\phi_B + \Theta,\ \phi_B - \Theta]$ the experimentally resolved reflectance has been evaluated in the vicinity of ϕ_{pB} and at slight offset $\Delta\phi_0 \in [\phi_B + \Theta,\ \phi_B - \Theta]$ [23]. For a divergence of the HeNe laser beam of ~ 1 mrad and depolarization of the p-polarized laser beam to for the HeNe laser and a depolarization of the p-polarized beam upon passage through the entrance window of the UHV growth chamber to $I_s/I_p = 10^{-6}$, the combined error in R_{po} is estimated to be $\sim 8 \times 10^{-6}$. Taking an error of 1 K in setting the growth temperature to 623 K, $\partial\varepsilon_3/\partial T \approx 10^{-3}$ and $\partial\varepsilon_4/\partial T \approx 3 \times 10^{-3}$, an error of 2.7×10^{-6} is added, which is negligible compared to the error caused by even small errors in setting ϕ_1 e.g. $\delta R_{po} \approx 10^{-4}$ for $\phi_1 - \phi_{pB} = 0.3°$ [23]. With care, it should be possible to set ϕ_1 with an accuracy of 0.05°.

4. Challenges in controlling non-steady-state and high pressure growth processes

Since in the early stages of nucleation and overgrowth of a substrate by a heteroepitaxial film the separation of film growth from the surface kinetics by linearization (Eq. (5)) is no longer valid, the modeling of the growth of high resolution heterostructures is far more difficult than the modeling of steady-state growth. This difficulty is further enhanced by differences between the decomposition rates of source vapors and transport rates of products on the epilayer and substrate surface elements during the nucleation period before coalescence of the nuclei into a contiguous heteroepitaxial film. Since, in addition to inhomogeneities in the composition of the SRL in the initial stages of overgrowth, the corrugation of the epilayer during the same period results in deviations of its dielectric function from the bulk value, the modeling of the formation of high resolution heterostructures represents an exceedingly complex task that requires detailed knowledge of the kinetics of the nucleation and coalescence process. Shortening this period as much as possible and keeping the surface roughness during the nucleation and coalescence process to a minimum are thus important goals of the control of the heteroepitaxial process.

Fortunately, real-time optical monitoring in conjunction with LLS measurements and other supplementing techniques, such as on-line atomic probe microscopy/spectroscopy, provide valuable guidance in realizing optimum conditions. For example, we have shown that by increasing the TEG flux in the first 1-–5 s of the nucleation period for GaP on Si(100) signatures of three-dimensional growth in R_{po} can be suppressed to values that are small on the scale of the fine structure [17,18]. Also, we have performed atomic force studies of the Si surface at various stages of the coalescence of nuclei into a contiguous epitaxial film that reveal the correlation of the structure observed in the PR signal to the nucleation and coalescence process [24]. Fig. 5 shows AFM line scans over a distance of 5 μm on the surface of a Si(100) substrate for (a) the initial hydrogen-terminated

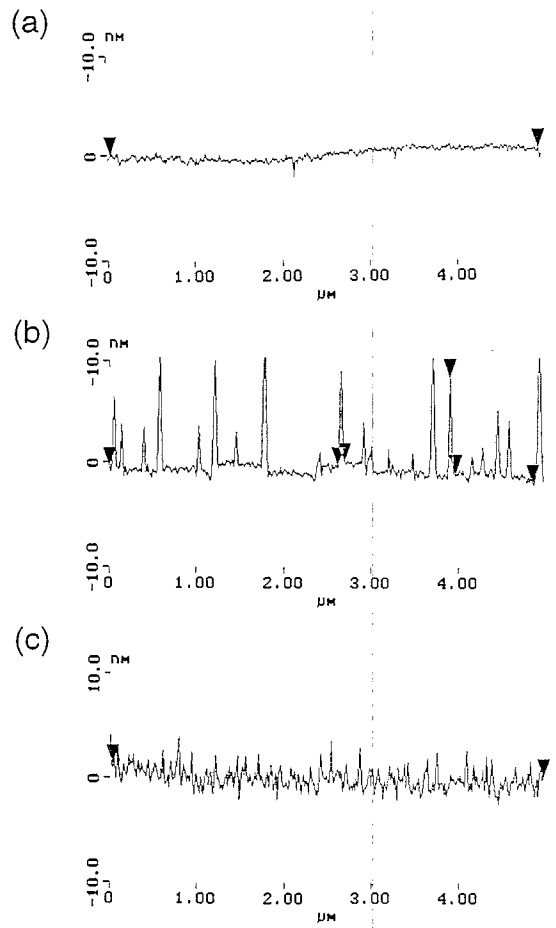

Fig. 5. Top: AFM line scans over a length of 5 μm on the surface of a Si(100) wafer (a) prior to heating to the growth temperature, (b) after 20 s of exposure to TEG and TBP pulses and (c) after 40 s of exposure to TEG and TBP pulses. Bottom: plot of the PR intensity versus time for an exposure of 80 s to TEG and TBP pulses.

surface, (b) 20 s into the nucleation period and (c) after coalescence of the nuclei into a contiguous film. The nuclei at the stage of lateral growth represented in Fig. 5(b) are 50–100 nm wide and 2–10 nm high, that is, corresponding to a Volmer–Weber type nucleation and overgrowth mechanism in this particular case. This is revealed in the PR signal by an increased amplitude of R_{po} due to the smaller value of the effective dielectric constant ε_{3eff} for the corrugated GaP film as compared to the bulk dielectric constant ε_3 of GaP [18]. Typically this feature merges into the interference oscillations for the bulk film after 30–40 s. The simultaneous control of film thickness and composition by PR measurements is possible in principle on the basis of measurements at two angles of incidence at constant wavelength [25]. However, ultimately the control of the heteroepitaxial overgrowth process must include the simultaneous analysis of the line shape of the fine structure and slope S_e, which contain information concerning the composition of the SRL and the kinetics of the growth process [18,20].

Another aspect of engineered MLE that deserves evaluation is the extension of the processing technology to higher vapor densities, affording advances in throughput and improvements in the control of compound stoichiometry. The latter is particularly important for compounds that exhibit high decomposition pressure e.g.

heteroepitaxial growth of $Ga_xIn_{1-x}N$. Both intensity fluctuations and bending of the incident laser beam represent possible limitations to the precision and accuracy of PR real-time monitoring, respectively. They are caused by fluctuations in the vapor density, resulting in scattering losses, and by the temperature gradient in the vicinity of the substrate surface, resulting in a gradient in vapor density. Preliminary experimental evaluations of the noise in the PR signal under the conditions of high pressure vapor transport [26], for a HeNe laser beam reflected from a GaP surface in a nitrogen atmosphere, show that in the range between 573 and 673 K, the noise at 5 bar pressure is approximately one order of magnitude higher than that measured under the conditions of PCBE. Thus the engineering of MLE growth of nearly lattice-matched III–V heterostructures on Si under conditions of high pressure vapor epitaxy may be severely curtailed. However, the resolution still remains at sub-molecular layer level and should suffice for process control in the context of the fabrication of a variety of heterostructures for which this resolution is adequate e.g. the deposition of dielectric mirrors and wave guides. Whether PR represents a sufficient advantage in such applications to replace finger printing methods based on near normal incidence reflectance measurements is not clear at present, because of the higher complexity of implementing PR, and requires further evaluation. We can note, however, that in applications, where the ambient is at relatively high pressure it may be necessary to rely on reflectance rather than phase-sensitive techniques, such as SE, since the phase is much more sensitive to density fluctuations than the intensity.

5. Conclusions

Based on the above results we conclude that engineered MLE is possible at this time under the conditions of PCBE for selected materials systems with a precision of a few per cent. However, the requirement of long source vapor cycle time prevents gains in throughput as compared to self-limiting mechanisms of MLE. Also, potential gains in throughput from operation of chemical vapor deposition processes at higher nutrient densities are compensated by increases in noise. Challenging problems exist in the control of non-steady-state growth, particularly under conditions of nucleation and coalescence that are accompanied by inhomogeneous surface chemistry and surface roughening. However, PR and related reflectance spectroscopies provide valuable guidance in addressing these challenges. The simultaneous monitoring of film composition and thickness by PR is possible on the basis of measurements at two angles of incidence. Simultaneous analyses of the fine structure and slope of the PR signal represents an alternative approach to control, but requires progress in relating the fine structure directly to the growth kinetics, which depends on breakthroughs in the theoretical description of the dielectric function of the SRL in terms of the activities of its constituents. The best prospects for future developments of real-time control of chemical vapor deposition and etching processes are provided by combinations of real-time optical monitoring techniques, such as SE, PR, LLS and reflectance difference spectroscopy, which in principle allow the simultaneous assessment and control of growth at the process (ambient), SRL, and product (sample) levels and directly determining the sample properties, such as thickness, composition, surface roughness, composition and structure.

References

[1] T. Suntola and J. Antson, Finnish Patent 52359 (1974).
[2] T. Suntola, Mater. Sci. Rep. 4 (1989) 261.
[3] Y. Suda, D. Lubben, T. Motooka and J.E. Greene, J. Vac. Sci. Technol. B 7 (1990) 1171.
[4] T.A. Pakkanen, V. Nevalainen, M. Lindblad and P. Makkonen, Surf. Sci. 188 (1987) 456.
[5] K.P Killen and W.G. Breiland, J. Electron. Mater. 23 (1994) 179.
[6] J.C. Bean, L.J. Peticolas, R. Hull and D.L. Windt, Appl. Phys. Lett. 63 (1993) 444.
[7] N. Dietz and K.J. Bachmann, Mater. Res. Bull. 20 (1995) 49.
[8] N. Dietz and K.J. Bachmann, Vacuum 47 (1996) 133.

[9] D.E. Aspnes, W.E. Quin and S. Gregory, Appl. Phys. Lett. 56 (1990) 2569.
[10] R.H. Hartley, M.A. Folkard, D. Carr, P.J. Orders, D. Rees, I.K. Varga, V. Kumar, G. Shen, T.A. Steele, H. Buskes and J.B. Lee, J. Vac. Sci. B 10 (1992) 1410.
[11] G.N. Maracas, J.L. Edwards, D.S. Gerber and R. Droopad, Appl. Surf. Sci. 63 (1993) 1.
[12] D.E. Aspnes, W.E. Quin, M.C. Tamargo, M.A.A. Pudensi, S.A. Schwartz, M.J.S.P. Basil, R.E. Nahory and S. Gregory, Appl. Phys. Lett. 60 (1992) 1244.
[13] J.T. Kelliher, A.E. Miller, N. Dietz, S. Habermehl, Y.L. Chen, Z. Lu, G. Lucovsky and K.J. Bachmann, Appl. Surf. Sci. 86 (1995) 453.
[14] N. Dietz, A.E. Miller and K.J. Bachmann, J. Vac. Sci. Technol. 13 (1995) 153.
[16] N. Dietz, U. Rossow, D.E. Aspnes and K.J. Bachmann, J. Electron. Mater. 24 (1995) 1571.
[17] K.J. Bachmann, U. Rossow and N. Dietz, Mater. Sci. Eng. B 37 (1995) 478.
[18] K.J. Bachmann, U. Rossow, N. Sukidi, H. Castleberry and N. Dietz, J. Vac. Sci. Technol. B 14 (1996), in print.
[19] S.P.F. Humphrey-Owens, Proc. Phys. Soc. 87 (1961) 949.
[20] U. Rossow, N. Dietz, K.J. Bachmann and D.E. Aspnes, J. Vac. Sci. Technol. B 14 (1995), in print.
[21] M. Cardona and G. Harbeke, in: Landolt-Börnstein, Numerical Data and Functional Relationships in Science and Technology, New Series, Vol. 17 (Springer-Verlag, Berlin, 1982) p. 208.
[22] P. Lautenschlager, M. Garriga, L. Viña and M. Cardona, Phys. Rev. B 36 (1987) 4821.
[23] N. Dietz and H.J. Lewerenz, Appl. Phys. Lett. 59 (1991) 1470; 69 (1993) 350.
[24] A.E. Miller, M.Sc. thesis, Department of Materials Science and Engineering, North Carolina State University, Raleigh, North Carolina, July (1996).
[25] R.M.A. Azzam, J. Opt. Soc. Am. A 6 (1989) 1213.
[26] S. Fiechter, R.H. Castleberry, N.A.L. Dietz, K.J. Bachmann, H.T. Tran, K. Ito and J.S. Scroggs, Proc. 7th Int. Symp. on Experimental Methods for Microgravity Materials Science, ed. R.A. Schiffman, TMS, Warrendale, PA (1995) p. 5712.